

## RARAF – Table of Contents

<b>RARAF Professional Staff and Picture</b> .....	117
<b>Research using RARAF</b> .....	117
<b>Development of Facilities</b> .....	118
<b>Singletron Utilization and Operation</b> .....	121
<b>Training</b> .....	125
<b>Personnel</b> .....	126
<b>Recent Publications of Work Performed at RARAF</b> .....	128

## RARAF PROFESSIONAL STAFF



**RARAF Staff (l-r):** Alan Bigelow, Charles Geard, Sasha Lyulko, Andrew Harken, David Brenner, Yanping Xu, Guy Garty, Stephen Marino, Hamin Jeon and Gerhard Randers-Pehrson. Not shown: Antonella Bertucci, Brian Ponnaiya, Helen Turner and Gary Johnson.

**David J. Brenner**, Ph.D., D.Sc. – CRR Director, RARAF Director  
**Stephen A. Marino**, M.S. – RARAF Manager  
**Gerhard Randers-Pehrson**, Ph.D. – RARAF Associate Director, Chief Physicist  
**Charles R. Geard**, Ph.D. – Senior Biologist  
**Guy Y. Garty**, Ph.D. – Research Scientist  
**Alan Bigelow**, Ph.D. – Associate Research Scientist  
**Brian Ponnaiya**, Ph.D. – Associate Research Scientist  
**Helen Turner**, Ph.D. – Associate Research Scientist  
**Antonella Bertucci**, Ph.D. – Associate Research Scientist  
**Andrew D. Harken**, Ph.D. – Post-Doctoral Research Scientist  
**Yanping Xu**, Ph.D. – Post-Doctoral Research Scientist  
**Oleksandra Lyulko**, – Pre-Doctoral Research Scientist

# The Radiological Research Accelerator Facility

AN NIH-SUPPORTED RESOURCE CENTER – WWW.RARAF.ORG

*Director: David J. Brenner, Ph.D., D.Sc.*

*Associate Director: Gerhard Randers-Pehrson, Ph.D.*

*Manager: Stephen A. Marino, M.S.*

## Research Using RARAF

The “bystander” effect is the response of cells that are not directly irradiated when in close contact with, or are even only in the presence of, irradiated cells. For the past several years, many of the biology studies, including those involving animals, have examined this effect. The emphasis of most of the present experiments is to determine the mechanism(s) by which the effect is transmitted, primarily direct gap junction communication through cell membrane contact. Both the Microbeam and the Track Segment Facilities continue to be utilized in various investigations of this phenomenon. The single-particle Microbeam Facility provides precise control of the number and location of particles so that irradiated and bystander cells may be distinguished, but is somewhat limited in the number of cells that can be irradiated. The Track Segment Facility provides broad beam irradiation that has a random pattern of charged particles but allows large numbers of cells to be irradiated quickly.

To investigate cell-to-cell communication in the bystander effect using the Track Segment Facility a special type of cell dish is used. These “strip” dishes consist of a stainless steel ring with thin Mylar foil glued to one side into which a second, slightly smaller dish is inserted. The Mylar foil glued to the inner dish has alternate strips of the Mylar removed. Cells are plated over the combined surface and are in contact. The Mylar on the inner dish is thick enough (38  $\mu\text{m}$ ) to stop the  $^4\text{He}$  ions and the cells plated on that surface are not irradiated and are “bystander” cells.

Research into bystander effects in 3-D systems continued this past year. Cultured tissue samples were irradiated in a thin line with either helium ions or protons using the Track Segment Facility. A prototype fixture has been constructed and tested that would allow microbeam irradiation of the very thin ears of hairless mice. Another fixture has been tested that would enable the rapid irradiation of multiple *C. elegans* nematodes without anesthetization. The multiphoton laser system has been used to image zebrafish hatchlings in preparation for future microbeam irradiations by William Dynan at the Georgia Health Sciences University.

The multiphoton laser system is a tool that can be used independently of the charged particle microbeam to produce 3-D images of specimens or to irradiate them with the UV microspot. Several users, both internal and external, have begun to make use of this facility, particularly for 3-D imaging.

The experiments performed using the RARAF Singletron between January 1 and December 31, 2010 and the number of shifts each was run in this period are listed in Table I. Fractional shifts are assigned when experimental time is shared among several users (*e.g.*, track segment experiments) or when experiments run for more or less than an 8-hour shift. Use of the accelerator for experiments was 20% of the regularly scheduled time (40 hours per week), about 1/3 lower than last year. Twelve different experiments were run during this period. Five experiments were undertaken by members of the CRR, supported by grants from the National Institutes of Health (NIH) and the National Aeronautics and Space Administration (NASA). Seven experiments were performed by external users, supported by grants and awards from the Department of Defense (DoD), NASA, and the Department of Energy (DoE). Brief descriptions of these experiments follow.

Efforts to identify the cell-to-cell signaling transduction pathways involved in radiation-induced bystander responses were continued by Hongning Zhou and Tom Hei of the CRR (Exp. 110). In some experiments a fraction of the cells were irradiated either in the nucleus or the cytoplasm using the Microbeam Facility focused  $^4\text{He}$  beam. Induced micronucleus formation in COX-2 wild type or heterozygote mouse embryo fibroblasts was significantly higher than in controls; however in COX-2 null mouse embryo fibroblasts this bystander response was dramatically reduced after either nuclear or cytoplasmic irradiation. Cytoplasmic irradiation induced mutagenesis in mitochondrial functional human skin fibroblasts, although the mutation induction was relatively lower than in the nuclear-irradiated cells. It induced, however, very little, if any, mutagenesis in directly irradiated cells without mitochondrial DNA. Furthermore, using real-time quantitative PCR they found that cytoplasmic irradiation with  $^4\text{He}$  ions induced a transient increase in mitochondrial DNA content in human skin fibroblasts as a function of time post irradiation. One day post-irradiation, cells were stained with DiOC6, a cell-permeant, green fluorescent dye that is selective for the mitochondria of live cells. When compared to similarly-treated controls, irradiated cells showed a significant reduction in mitochondrial membrane potential, indicating a loss of function. These results indicate that mitochondria play a critical role in cytoplasmic

irradiation-induced genotoxicity and have implication for understanding the cellular response to DNA damage and low-dose radiation risk assessment.

Military personnel can be exposed to the radioactive alpha emitter and heavy metal depleted uranium (DU). Alexandra Miller of the Armed Forces Radiobiological Research Institute (AFFRI) continued studies using 125 keV/ $\mu\text{m}$   $^4\text{He}$  ions from the Track Segment Facility to evaluate DU radiation-induced carcinogenesis using *in vitro* models and to test safe and efficacious medical countermeasures (Exp. 113). Human osteoblast cells (HOS) cells were irradiated with  $^4\text{He}$  ions using the Track Segment Facility to evaluate the effect of the biological countermeasure phenylbutyrate (PB). The following endpoints were examined: survival, neoplastic transformation, chromosomal aberrations, and global DNA methylation status. The results demonstrated that 1) alpha particle exposure induced DNA hypomethylation; 2) PB can protect HOS cells from alpha radiation-induced neoplastic transformation and chromosomal damage.

A group led by Sally Amundson of the CRR concluded three experiments using cDNA microarray hybridization and other methods to investigate radiation-induced gene expression profiles in primary human fibroblast and epithelial cell lines. Shanaz Ghandhi and Lihua Ming used the Track Segment Facility for comparison of gene expression responses to direct and bystander irradiation (Exp. 133). Human lung fibroblast cells (IMR90) and human skin fibroblasts were plated on "strip" dishes for direct-contact bystander irradiations using a dose of 0.5 Gy of 125 keV/ $\mu\text{m}$   $^4\text{He}$  ions. Cells were assayed for micro-nucleus formation and gene expression and western blot analysis was performed. A role for interleukin-33 in the signal transmission for the bystander effect was identified.

In the second experiment (Exp. 136), performed by Alexandre Mezentsev, artificial human tissue model Epi-200 (MatTek) was irradiated using the Track Segment Facility. The tissue is composed of ~20 layers of cells, which represent keratinocytes at different stages of differentiation. The goal of this project is to characterize the effects on tissue *ex vivo* of low and high doses of ionizing radiation. The tissues were irradiated with protons having an initial LET of ~10 keV/ $\mu\text{m}$  or  $^4\text{He}$  ions having an initial LET of ~73 keV/ $\mu\text{m}$ , either over the entire tissue surface or in a narrow line (~25  $\mu\text{m}$ ) across the diameter using a thin, slit-shaped collimator. Two types of procedures were performed: isolation of total RNA and immunohistochemistry. The RNA provides quantification of gene expression by Microarray analysis and validation by quantitative real-time PCR. Microarray results are analyzed by computer using gene ontology procedures and network analysis, which normally has a graphical output representing the specific responses to the ionizing radiation. Tissue samples are also fixed in formalin, embedded in paraffin, and sectioned parallel to the line of irradiation for immunohistochemistry and counterstaining. This provides characterization of proteins of interest and describes their role in post-

irradiation events, such as transcriptional regulation, contribution to cell signaling mechanisms, and gap junction signaling.

In the third experiment, Sally Amundson used the Microbeam Facility to irradiate primary human lung fibroblasts either in the nucleus or the cytoplasm with 5.2 MeV  $^4\text{He}$  ions. RNA was extracted at half-hour and four-hour post-exposure time points to perform global gene expression analysis in order to gain a better understanding of the cell signaling that arises from radiation damage to the cytoplasm and which damage response pathways require direct damage to DNA (Exp. 139). Results of the experiments have been unexpected; repeated irradiations have been performed and additional controls have been examined to confirm these results.

David Chen and Aroumougame Asaithamby from the University of Texas Southwestern Medical Center extended their work on DNA damage sensing and repair factors to the investigation of base-damage-repair dynamics in HT1080 human fibrosarcoma cells after microbeam irradiation (Exp. 141). The cells contain enhanced green fluorescent protein (EGFP) reporter attached to the base-repair protein 8-oxoguanine DNA glycosylase 1 (OGG1). As a preliminary step to microbeam irradiation, it was decided to verify that UV laser induction of OGG1 foci at UT Southwestern also could be observed at RARAF. The multiphoton microscope at RARAF was used in two modes: as an imaging device and as a UV microspot irradiator. For pre- and post-irradiation multiphoton microscopy imaging, 970 nm incident laser light, which acts as 485 nm during two-photon excitation, was used to excite EGFP. For UV microspot irradiation, the laser was tuned to 700 nm incident laser light, which acts as 350 nm at the microspot, to induce DNA damage in the cell nuclei. It was observed that when the laser energy delivered to a cell nucleus was excessive, the cell nucleus was virtually annihilated. When the delivered energy was reduced below the cell-killing threshold, OGG1 foci formation was observed along with an intact cell nucleus, verifying laser-induced UV OGG1 foci formation.

A study of the LET dependence of DNA fragmentation using the Track Segment Facility was undertaken by Dalong Pang of Georgetown University (Exp. 147). Viral plasmids in solution were made into a thin layer of known thickness by pipetting a small volume onto a standard track segment dish, placing a cover slide on the liquid, and forcing the liquid to the edges of the cover slip. The DNA was irradiated with doses from 1kGy to 8 kGy of 10 keV/ $\mu\text{m}$  protons or 73 or 125 keV/ $\mu\text{m}$   $^4\text{He}$  ions. The irradiated DNA samples were subsequently analyzed using the atomic force microscope at Georgetown University. The DNA fragment lengths were measured and grouped into various length intervals, and length-dose histograms were constructed. From the histograms, quantities such as the number of DSB per DNA and the spatial distribution of double-strand breaks (DSB) on a DNA molecule were derived. The LET dependence of these quantities was observed, indicating

the greater clustering capacity of high-LET radiations. Monte Carlo simulation of DNA fragment length distribution by the aforementioned radiations is underway and the results will be analyzed in comparison to the AFM measured data. Further validation and refinement of the model may be achieved through such comparisons. The biological significance of short DNA fragments in non-homologous end joining (NHEJ) generated by clustered DNA damage is being investigated using DNA binding, kinase activation, and rejoining assays. Proteins examined include Ku, DNA-PK, and DNA ligases.

A new wide-energy neutron spectrometer design, intended for use in the International Space Station to examine the neutron spectrum to which astronauts are exposed, was tested at RARAF by David Slaughter of Photogenics (Exp. 149). The spectrometer consists of a large plastic scintillator containing  ${}^6\text{LiGd}(\text{BO}_3)_3\text{:Ce}$ . Some of the neutrons lose all their energy in multiple collisions in the scintillator, producing an initial light pulse in the scintillator. The residual neutron is captured by  ${}^6\text{Li}$ ,  ${}^{10}\text{B}$ , or natural Gd, which all have extremely large thermal neutron capture cross sections. The nucleus that has captured the neutron releases an energetic alpha particle or electron producing a second pulse in the detector, which indicates that the first pulse constituted the entire neutron energy. An advantage of this design is the direct measurement of the neutron spectrum. Most other spectroscopy systems require complicated deconvolution programs to determine the neutron spectrum. Spectrum measurements were made for neutron energies between 0.5 and 2.5 MeV as well as 5.9 and 14.0 MeV. The chamber was also irradiated with  $\sim 4.2$  MeV protons to observe individual proton pulses.

A broad-beam charged particle facility has been developed at the LARN Laboratory at the University of Namur, Belgium. Stephané Lucas initiated an intercomparison of the LARN and RARAF irradiation facilities (Exp. 148). Three graduate students from the University of Namur assisted in performing the cell irradiations. Cell survival after irradiation of the cancer cell line A549 at RARAF with  ${}^4\text{He}$  ions at dose rates similar to those used at LARN indicated a much greater cell killing than at the Belgian facility ( $\alpha = 3.3$  vs. 2.4). Interestingly, they observed that irradiated EAhy926 endothelial cells, when co-cultured with un-irradiated A549, induced a significant mortality in the A549 cells, which was almost as high as observed after A549 cell irradiation. To better understand the interaction between the two cell types after irradiation, a gene expression analysis was performed using Taqman Low Density Arrays. Interestingly, p21 was not overexpressed by EAhy926 cells 24h after 1 Gy  ${}^4\text{He}$  ion irradiation. The expression of GADD45A also did not change. This may suggest that p53 was not activated after EAhy926 cell irradiation or that the activation occurs earlier.

Measurements of cell and nucleus thicknesses were made for confluent and non-confluent A549 cells using the multiphoton microscope and staining with Hoechst 33342(nucleus), CellTracker Orange and CellMask Orange (cytoplasm and membrane).

David Cove, from the University of Leeds, UK and Ralph Quatrano from Washington University in St. Louis, where Dr. Cove was visiting, irradiated the moss *Physcomitrella patens* to produce mutant spores by charged particle irradiation using the Track Segment Facility (Exp. 150). He was assisted by Edward Tucker of Baruch College, CUNY, who actually performed the irradiations and had performed charged particle irradiations of the same moss at RARAF several years ago (Exp. 127). Ion beam irradiation is reported to induce DNA deletions up to about 10kb. Using arrays, the sequence deleted from the genome can be detected. The aim is to establish a procedure for the identification of genes, mutations in which lead to specific phenotypes. If this procedure could be made routine, it would open up a path to forward gene discovery, which is at present not available for this model system. Unfortunately, initial experiments to determine a survival curve for 10 keV/ $\mu\text{m}$  protons suffered from contamination and erratic response.

An investigation into adaptive and bystander effects in the human colon cancer cell line HCT116 was initiated by David Boothman of the University of Texas Southwestern Medical Center (Exp. 151). Cells with either both genes or neither gene for p53 (p53<sup>+/+</sup> or p53<sup>-/-</sup>) were transfected with either insulin-like growth factor-1 (IGF-1) or clusterin (CLU), both tagged with green fluorescent protein (GFP), and irradiated with the charged particle microbeam and the Track Segment Facility. After irradiation, cells were examined for GFP foci to determine if there was a response to DNA damage by either of the tagged proteins. In these initial irradiations, an elevated GFP expression as a function of dose was not observed for the three cell types which had retained sufficient cells to justify imaging. Further work needs to be done to get these cell lines to attach to and grow on the microbeam and track segment dishes and in staining the cells sufficiently for microbeam irradiation.

Brian Ponnaiya and Howard Lieberman of the CRR, with the assistance of Shanaz Ghandhi, are studying the effect of Rad9 on radiation-induced changes in gene expression in human and mouse cells directly irradiated or as bystanders (Exp. 152). Human H1299 cells that have Rad9 knocked down and mouse ES cells that have a homozygous deletion of Rad9, along with wild type controls, are being irradiated on strip dishes using the Track Segment Facility. Optimal doses of  ${}^4\text{He}$  ions in the range of 0.5 to 5 Gy are being determined by pilot studies. Cells will be collected at appropriate times after exposure up to 24 hours for gene expression analyses and micronucleus formation.

Table I. Experiments Run at RARAF January 1 - December 31, 2010

Exp No.	Experimenter	Institution	Exp. Type	Title of Experiment	Shifts Run
110	H. Zhou, T. K. Hei	CRR	Biol.	Identification of molecular signals of alpha particle-induced bystander mutagenesis	16.0
113	A. Miller	AFRRI	Biol.	Role of alpha particle radiation in depleted uranium-induced cellular effects	0.3
133	S. Ghandhi, S. Amundson	CRR	Biol.	Bystander effects in primary cells	4.0
136	A. Mezentsev S. Amundson,	CRR	Biol.	Bystander effects in 3D tissues	2.5
139	S. Amundson	CRR	Biol.	Signal transduction in cytoplasmic irradiation	3.5
141	A. Asaithamby D. Chen	Univ. of Texas Southwestern Medical Center	Biol.	Visualization of recruitment of DNA damage markers to the sites of DNA damage induced by microbeam irradiation	3.5
147	D. Pang	Georgetown Univ.	Biol.	LET dependence of DNA fragmentation by charged particles	8.5
148	S. Lucas	Univ. of Namur, Belgium	Biol.	Site comparison of two cell line irradiation with broad beam	3.0
149	D. Slaughter	Photogenics	Phys.	Characterizing a high-performance neutron spectrometer between 1-14 MeV using a LGB/PVT composite scintillator and PMT	3.5
150	D. Cove	Washington University	Biol.	Ion beam mutagenesis of the moss <i>Physcomitrella patens</i>	1.8
151	D. Boothman	Univ. of Texas Southwestern	Biol.	Role of ATM-IGF-1-sCLU in adaptive and bystander effects in human cancer cells.	1.8
152	B. Ponnaiya, H. Lieberman	CRR	Biol.	The role of Rad9 in mediating global gene expression in directly irradiated and bystander cells	0.8

### Development of Facilities

Development continued or was initiated on a number of extensions of our facilities:

- Focused accelerator microbeams
- Focused x-ray microbeam
- Neutron microbeam
- Non-scattering particle detector
- Advanced imaging systems
- Targeting and manipulation of cells
- Small animal systems

#### Development of focused accelerator microbeams

The electrostatically focused microbeam has been operating reliably for the past year, consistently producing a beam spot 1-2  $\mu\text{m}$  in diameter using a 500 nm thick silicon nitride exit window. This window has a larger area (1.5 mm x 1.5 mm), making it more useful for most irradiations than the thin (100 nm) window with dimensions of only 0.25 mm x 0.25 mm that is used when a sub-micron beam spot is desired.

Emphasis this year was on increased quality control and making the Microbeam a turn-key facility. Analog-to-digital converters were set up to monitor the control voltages to the six high voltage power supplies for the electrostatically focused charged particle microbeam, the output voltages and currents from those supplies, and the vacuum pressure at the upper electrostatic lens. This enables us to better diagnose any problems that might

occur with the lens rods. We now do a microbeam test run the evening before an irradiation. The next morning, after the accelerator has warmed up, the charged particle beam is found immediately and has a minimal beam spot diameter. This provides an earlier and trouble-free start for irradiations and consequently a greater throughput.

Because of damage to the quadrupole triplet rods in one of our compound lens systems in November 2009, 12 new ceramic quadrupole triplet rods were machined in our shop, a very painstaking and time-consuming process due to the precision required and the difficulty of machining ceramics. They were sent to the Institute of High Current Electronics in Russia in November for implantation of platinum ions to increase the surface resistivity, which reduces ion charge build-up on the insulating sections between the electrodes. The rods will return in early 2011. They will then be cleaned, the conductivities measured, the insulating sections carefully masked, and then sent out to have a gold layer 1  $\mu\text{m}$  thick plated on the electrode sections of the rods to make them conducting. The rods will be tested in vacuum with high voltage using the new test fixture constructed last year. After testing, eight of the rods will be assembled into two quadrupole triplet lenses and the lenses mounted in an alignment tube for insertion into the microbeam beam line where the voltages on the lens elements will be adjusted to produce a beam spot with the smallest diameter.

The permanent magnet microbeam (PMM) uses a compound quadrupole triplet lens made from commercially available precision permanent magnets. Its design is similar to that for the lens system for the sub-micron microbeam, the major difference being that it uses magnetic rather than electrostatic lenses. It consistently has been able to produce a  $^4\text{He}$  beam spot 5  $\mu\text{m}$  in diameter and in early 2010 it was used for microbeam irradiations when the lenses for the electrostatic microbeam were being worked on. The quadrupole magnet strengths used to focus the beam have been adjusted to produce a focused 4.4 MeV proton beam, which will be used with the Point and Shoot system to develop the Fast and Shoot microfluidics system described below.

#### Focused x-ray microbeam

We have developed an x-ray microbeam to provide characteristic  $K_{\alpha}$  x rays generated by proton-induced x-ray emission (PIXE) from Ti (4.5 keV). Charged particle beams can generate nearly monochromatic x rays because, unlike electrons, they have a very low bremsstrahlung yield.

A small x-ray source is produced by bombarding a Ti target with 1.8 MeV protons using a quadrupole quadruplet lens to focus the beam to  $\sim 50 \times 120 \mu\text{m}$  on the target, reducing the requirements on the subsequent x-ray focusing system. The x rays used are emitted at  $90^{\circ}$  to the proton beam direction. The target is at an angle of  $70^{\circ}$  to the proton beam, reducing the apparent size of the beam spot in the vertical direction to  $\sim 50 \times 50 \mu\text{m}$ . A zone plate is used to focus the x-ray source to a beam spot 5  $\mu\text{m}$  in diameter. The system is mounted on its own horizontal beam line on the 1<sup>st</sup> floor of RARAF and the x-ray beam is oriented vertically, so that the geometry of the microscope and stage is the same as for our charged particle microbeam systems. The diameter of the angle limiting aperture in front of the quadruplet lens has been increased, increasing the beam transmission by a factor of 4. By adjusting the lens voltages, the beam spot size was maintained.

New quadruplet rods have been machined in our shop, implanted with platinum ions, and the electrodes plated with gold. They have been tested to 10 kV using the lens rod test system and assembled into a new quadrupole quadruplet lens. This lens has an 8mm bore, significantly larger than the 2 mm bore on the existing quadruplet, which will allow much higher beam currents to be obtained greatly increasing the dose rate. The new lens has ground planes between each set of electrodes (5), providing better definition of the electric field than the previous lens, which only had ground planes at the ends and between the 2<sup>nd</sup> and 3<sup>rd</sup> elements (3).

#### Neutron microbeam

Neutrons produced by the  $^7\text{Li}(p,n)^7\text{Be}$  reaction are emitted only in a forward conical volume when the proton energy is just above the reaction threshold (1.881 MeV). The half-angle of this cone is dependent on the proton

energy and increases with increasing energy. A focused proton microbeam 5  $\mu\text{m}$  in diameter will be incident on a 1  $\mu\text{m}$  thick lithium fluoride target. The backing material will be 20- $\mu\text{m}$  thick Au, selected for its high density and thermal conductivity, which will stop the incident proton beam. Using a 1.886 MeV proton beam, thin samples in contact with the target backing will be exposed to a beam of neutrons 10-15  $\mu\text{m}$  in diameter having energies from 10-50 keV. This will be the first neutron microbeam in the world.

The facility is being constructed on a horizontal beamline using a quadrupole quadruplet to focus the proton beam to  $\sim 10 \mu\text{m}$  D. LiF targets have been obtained and construction is underway on the endstation and stage. The microscope, video camera and computer systems are being assembled and tested.

#### Non-scattering particle detector

Presently the RARAF microbeam endstation delivers a precise number of particles to thin samples by counting the particles traversing them using a gas proportional counter placed immediately above the cells. Because the  $^4\text{He}$  ions have a very short range ( $\leq 50 \mu\text{m}$ ), the medium over the cells must be removed to count the ions. To irradiate samples thicker than the range of the incident ions or to allow cell medium to remain in place during cell irradiations, a very thin particle detector is necessary between the beam exit window and the samples.

Development continued on an under-dish detector design that was initially investigated several years ago. An aluminum electrode was evaporated on one side of a thin silicon wafer and three parallel gold electrodes were evaporated on the opposite side, with only a small horizontal gap between the ends of the electrodes. The center gold electrode collects the charge in the diagonal region between it and the aluminum electrode on the opposite surface of the silicon. The other two gold electrodes are guards to reduce noise. Because the gap between the electrodes is much larger than the thickness of the wafer, the capacitance, and therefore the noise, is much lower than it would be if the electrodes overlapped. We have been unable to obtain wafers thinner than 10  $\mu\text{m}$ . Efforts to thin down these wafers to  $\sim 2 \mu\text{m}$  have been unsuccessful. The prototype detector produced a usable signal, but was too fragile for use, even with a 10  $\mu\text{m}$  thickness, and quickly broke.

Other thin detector designs are being investigated. One design involves amorphous silicon deposited on the surface of a silicon nitride microbeam vacuum window. Another design is to implant nitrogen ions into a thin piece of silicon, etch the silicon from the opposite side leaving the silicon nitride layer formed by the stopped nitrogen ions and a 1-3  $\mu\text{m}$  thick silicon layer on the implanted side. These designs are being developed in collaboration with the Mechanical Engineering Department of Columbia University and Michael Bardash at QEL, Inc.

Advanced imaging systems

New imaging techniques to view cells without using stain and to obtain three-dimensional images of unstained cells are of great importance for the microbeam irradiation facilities in order to avoid damage to the cells, to maintain physiological conditions, and to image thick samples, especially small animals, for targeting and observation.

Immersion-based Mirau interferometry (IMI) was developed at RARAF. An objective was constructed to function as an immersion lens using standard interferometric techniques by acquiring successive images at four positions with sub-wavelength separations using the vertical motion of the microbeam stage. It uses 540 nm (green) light for imaging and therefore does not induce UV damage in the cells. Interferometry is very sensitive to vibrations, even as small as a fraction of a wavelength. Although this system provides usable images in a vibration-free environment; on the electrostatic microbeam endstation small vertical motions due to vibrations in the building greatly reduce the image quality. Passive and active systems to reduce these vibrations were unsuccessful.

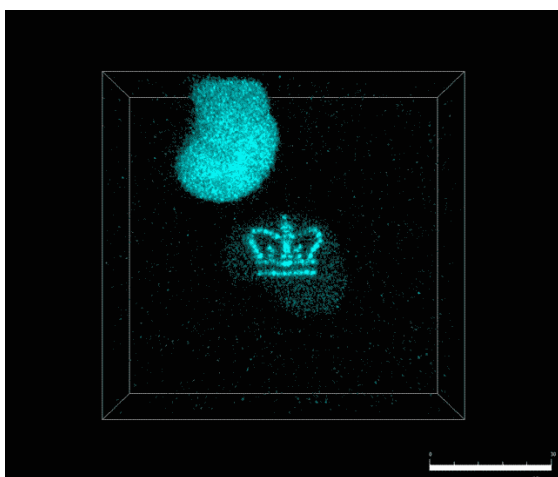


**Fig. 1.** Columbia crown logo formed in a single cell nucleus by laser UV microspot damage and visualized by fluorescent protein attached to single-strand DNA repair proteins.

In 2008, the feasibility of a new approach to overcome the vibration problem using Simultaneous Immersion Mirau Interferometry (SIMI) was demonstrated. Polarized light is split into equal components in the x and y planes, one of which undergoes a phase shift of  $90^\circ$  by use of  $1/8$  wavelength ( $\lambda/8$ ) waveplates. A polarization beam splitter is used to send the x and y components to form interferograms on a single camera. Since the images are taken simultaneously, there is no effect from the vibration. This system is also much faster than Immersion Mirau because only one image is necessary instead of four images at different distances, requiring 3 vertical

movements of the stage.

New optical elements are being fabricated to adapt the Immersion Mirau objective for Simultaneous Immersion Mirau Interferometry. The small, thin glass discs required (8 mm D, 0.2-0.3 mm thick) have been purchased and sent out to be coated, either as spot mirrors or partially reflective (10-85%) beam splitters. The discs will be assembled into 2- or 4-piece elements with  $1/8\lambda$  waveplates between the glass discs. When fabrication is completed, these elements will be placed in the objective lens housing and tested on the microbeam facility.

A multi-photon microscope was developed for and integrated into the microscope of the single-particle Microbeam Facility in 2007 to detect and observe the short-term molecular kinetics of radiation response in living cells and to permit imaging in thick targets, such as tissue samples. Two photons delivered closely together in space and time can act as a single photon with half the wavelength (twice the energy). This method has the advantages that the longer wavelength of the light beam allows better penetration into the sample while still being able to excite the fluorophor at the focal volume, and less damage is produced in the portion of the sample not in the focal volume.

The multiphoton system can also be used as a laser “microspot” to induce UV damage in the focal volume of the laser spot, a capability that some RARAF users have requested. A 3-D image of single-strand DNA damage induced in a single cell nucleus by the UV laser spot and imaged using the multi-photon laser is shown in Figure 1 and in 3D on the home page of the RARAF web site (raraf.org). The Columbia crown logo is the result of the fluorescence of tagged single-strand DNA repair proteins at sites of damage caused by the microspot in a single cell nucleus and imaged by multiple laser scans of the cell at different depths, producing a 3D image. As mentioned above, the multiphoton laser was used to produce and visualize DNA base damage in HT1080 human fibrosarcoma cells for the Chen group.

Targeting and manipulation of cells

A new targeting system based on microfluidics is being developed to increase the throughput of the microbeam. In the Flow And Shoot (FAST) system, cells moving through a narrow capillary are imaged by a high-speed camera to track their trajectory. The charged particle beam is deflected using the Point and Shoot system to the position of the cell on the trajectory and the particle beam is enabled. The deflection coil currents will be changed continuously to follow the path of the cell until the requested number of particles is delivered. The system will be capable of tracking several cells at a time. In addition to increasing the speed of the irradiations, this system will be able to irradiate non-adherent cells, such as lymphocytes, that do not plate on surfaces and therefore do not have stable positions.

For preliminary testing of cell flow and targeting we have manufactured a PDMS microfluidic chip using soft lithography. The cross-section of the channel has a width of 200  $\mu\text{m}$  and height of 20  $\mu\text{m}$ , so that the cells, when targeted by the microbeam, flow in the immediate vicinity of the exit window. The flow rate is controlled by a syringe pump. The chip itself is vacuum sealed to the microbeam exit window by applying the house vacuum ( $\sim 0.5$  atm) to a 1mm square cross chamber surrounding the flow channel. This reversibly holds the PDMS chip in place and seals the bottom of the flow channel without permanently bonding or gluing the channel to the window. Therefore, the channel can easily be cleaned or replaced to prevent contamination of biological experiments. The top of the irradiation section of the microfluidic channel is designed to be 20  $\mu\text{m}$  thick to let particles reach the detector above the channel. Further, we plan to integrate a nickel TEM grid above the channel to calibrate the beam size because the microfluidic channel does not permit traditional knife edge measurements. This chip has been used to test the microbeam cell tracking software.

Initial tests with fluorescent beads flowing through the channel and imaging at 25 frames/s using an image-intensified camera using resulted in errors in predicted bead position within 1  $\mu\text{m}$  90% of the time and within 2.5  $\mu\text{m}$  98% of the time. A fast camera has been ordered that will allow imaging at up to 1,000 frames/s. The increased imaging speed will make possible more accurate cell targeting and permit a higher flow rate, increasing throughput to as much as 100,000 cells/hr.

Another method for the irradiation of non-adherent cells is a novel cellular manipulation technique being adapted for the microbeam endstation at RARAF. We are developing an Optoelectronic Tweezer (OET) system, initially developed by our collaborators, the Ming Wu group at Berkeley National Laboratory. We have created a set of OET electrodes using the equipment provided in the clean room at Columbia University. As a preliminary test, we manufactured the devices on 1 mm thick glass slides. Future work will focus on reducing the thickness of the bottom substrate to allow charged particles to easily pass through.

The OET consists of two parallel-plate Indium Tin Oxide (ITO) electrodes. The top electrode is covered with a 1  $\mu\text{m}$  thick layer of hydrogenated amorphous silicon (a-Si:H), a thin-film semiconductor that acts as a photoconductive layer. When light is focused on the surface of the a-Si:H, the conductivity of the layer increases by several orders of magnitude. By patterning a dynamic light image on the electrode, a reconfigurable virtual electrode is created. When the virtual electrode and its opposing plate electrode are biased with an AC voltage, a non-uniform AC field is created.

In the presence of a non-uniform electric field, a dielectric particle (e.g., cell) will feel a force caused by dielectric polarization (dielectrophoresis, DEP). The

conductivity of the fluid in the chamber must be carefully controlled as it will strongly affect the electric field in the fluid layer of the OET “sandwich”. If the resistance of the fluid layer is less than that of the a-Si:H, then the voltage drop will occur in the a-Si:H layer, and the DEP effect will be reduced in the liquid. The direction of the force is a function of the AC voltage frequency and the fluid conductivity. Below a certain frequency the cells are attracted by the force; at higher frequencies they are repelled.

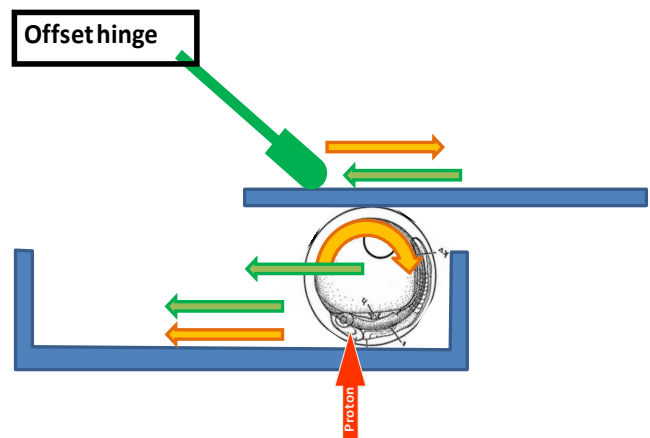


Fig. 2. Scheme of the fish embryo orientation system.

Initial tests have demonstrated the ability to manipulate fluorescent beads, moving them around with an image projected by a laser using the scanning mirror system constructed for multiphoton imaging. Future tests will be done using computer-generated images projected into the microscope.

#### Small animal systems

The advantages of *C. elegans* as a research tool are well-established, being a multi-cellular eukaryotic organism that is simple enough to be studied in great detail. From a practical perspective, it is small enough to be compatible with microbeam irradiation and a wide variety of mutants and transgenics are readily available as is a large community of *C. elegans* researchers.

In order to support high-throughput irradiations of *C. elegans* worms, we have developed, in collaboration with the Whitesides group at Harvard University, a microfluidic worm clamp for rapid immobilization of large numbers of live worms for morphological analysis and fluorescence imaging. The worm clamps manufactured for our use have four channels and a 10  $\mu\text{m}$  thick polydimethylsiloxane (PDMS) bottom to allow charged particle penetration. We have begun testing these chips for anesthetic-free irradiation of *C. elegans* worms and have seen that the worms indeed remain immobilized. Using this clamp, irradiations can be performed at much higher throughputs than with anesthetized worms, which need to be manually handled individually.

In our initial irradiations of medaka embryos, each embryo was oriented so that the eyes of the embryo were positioned just above the microbeam focal point. The medaka eggs (~ 1 mm D) were rolled around manually using a cover slip to get the correct orientation and the stage was moved to position them over the beam. This was a laborious and time-consuming procedure, which greatly limited the number of specimens that could be irradiated.

Orientation of the fish embryos is being automated using a combination of an offset hinge-mounted probe and the microbeam stage. When the stage and hinge are moved in the same direction (Figure 2), the embryo is translated (green arrows). When the offset hinge and microbeam stage are moved in opposite directions, the embryo is rotated (orange arrows).

In continuing our collaboration with William Dynan (Georgia Health Sciences University, Exp.143), we are investigating the extension of our previous work in irradiating medaka embryos to the irradiation of zebrafish hatchlings. Dr. Dynan has been developing transgenic strains of zebrafish with DNA strand break repair proteins, such as 53BP1, tagged with yellow fluorescent protein (YFP). The novelty of attaching YFP to DNA repair protein is that it enables real-time imaging of the DNA repair process. Following charged particle irradiation, for instance, repair protein converges on DNA damage sites. Subsequent images of YFP reveal foci that indicate the location of DNA damage-and-repair sites. Dr. Dynan's goal is to observe and measure the dynamics of radiation-induced foci formation in single-cell nuclei within live zebrafish hatchlings.

The proposed experiments involve 72-hour post-fertilization transgenic tagged hatchlings, where organ formation is largely complete and the hatchlings are optically clear except for the eyes. At this stage, the hatchlings are about 200  $\mu\text{m}$  thick and a few millimeters in length. During microbeam irradiations with protons, a hatchling will be anesthetized with Tricane. A thin layer of low-melting-point agarose will blanket the hatchling and hold it in place during primary imaging for targeting, irradiation, and follow-up imaging.

Since hatchlings differ significantly from the medaka embryos that we have worked with previously, initial work has involved 3D multiphoton imaging. Fixed hatchlings that were sent to RARAF were removed from their container by pipette and placed on a glass slide. Multiphoton z-stack images were acquired using a 10X objective. Each z-stack comprised 100 optical sections taken at 1- $\mu\text{m}$  increments. During our preliminary multiphoton microscopy trials, three imaging modes were observed: a) YFP fluorescence, b) second harmonic generation (SHG) signal, and c) autofluorescence signal. These initial imaging results are encouraging in that they offer several approaches to identifying potential targets within a hatchling. With higher magnification we will be able to distinguish single cells, observe radiation-induced foci formation in irradiated cells, and also investigate

potential bystander effects in non-targeted cell nuclei.

Several of our users have requested that a mouse skin model be adapted for microbeam irradiation. The chosen model is the SKH-1 hairless mouse ear system. The hairless mouse is a very standard model and the hairless mouse ear is also well established, having first been used in 1980. The ear of the young adult hairless mouse is transparent and large, measuring approximately 13 mm in both length and width, and with an average thickness of 250  $\mu\text{m}$ . Thus it is highly amenable to irradiation with our 5-MeV proton microbeam, which has a range of 350  $\mu\text{m}$ .

We designed and constructed a dedicated mouse and mouse ear holder for microbeam irradiation. The mouse holder is designed to safely restrain the animals as well as support the use of anesthetics during microbeam exposure and is based on a system originally developed in 1980 by Elof Eriksson for microscopic observation of microcirculation in the hairless mouse ear.

The next step was the testing of our customized microbeam mouse/mouse ear holder. The mouse was immobilized using a low-dose cocktail of ketamine/xylazine. The anesthetized mouse was laid on its back on a customized conical area of the mouse holder, while its head was sustained by a customized support. The ear of the anesthetized mouse was then flattened onto the underside of a flat plate using gentle suction provided by a vacuum system incorporated in our holder. This configuration was chosen because in this position the mouse ear can be located underneath the open window of the ear holder, where it can be irradiated by the microbeam.

All tests were conducted in an environment controlled for temperature and humidity. The mouse was kept under observation for 48 hours post test to evaluate whether any sign of discomfort was induced by the anesthesia and handling/restraint procedures. Preliminary results of the tests showed that our microbeam mouse holder does not interfere with the mouse physiology, providing a useful platform for precise manipulation and targeting of in vivo structures using proton microbeams.

### ***Singletron Utilization and Operation***

Table II summarizes accelerator usage for the past year. The Singletron is started between 7 and 7:30 a.m. on most days from September through June and between 8 and 9 a.m. the rest of the year. The nominal accelerator availability is one 8-hour shift per weekday (~250 shifts per year); however the accelerator is frequently run well into the evening, often on weekends, and occasionally 24 hours a day for experiments or development. During one period this year the accelerator was run continuously for 10 days.

Accelerator use for radiobiology and associated dosimetry was about 2/3 of that for last year. About half of the use for all experiments was for microbeam irradiations and 40% for track segment irradiations.

**Table II.**  
**Accelerator Use, January - December 2010**  
**Usage of Normally Scheduled Shifts**

<b>Radiobiology and associated dosimetry</b>	<b>18%</b>
<b>Radiological physics and chemistry</b>	<b>1.5%</b>
<b>On-line facility development and testing</b>	<b>46%</b>
<b>Safety system</b>	<b>2%</b>
<b>Accelerator-related repairs/maintenance</b>	<b>7%</b>
<b>Other repairs and maintenance</b>	<b>3%</b>
<b>Off-line facility development</b>	<b>30%</b>

Approximately 45% of the experiment time was used for experiments proposed by external users, about 3 times the percentage for last year and about twice the number of shifts.

On-line facility development and testing was almost half the available time, about the same as the average for the past 5 years. This was primarily for development and testing of the electrostatically focused microbeam, the PMM, and the x-ray microbeam.

There were 18 shifts of Singletron maintenance and repair time this year due to routine maintenance of the ion source and replacement of the RF tubes used to excite the ion source plasma. This is the same as the average since the Singletron was installed 5 years ago and probably represents the minimum maintenance required. The Singletron charging system continues to be very stable and reliable.

**Training**

We again participated in the Research Experiences for Undergraduates (REU) project this past summer, in collaboration with the Columbia University Physics Department. Students attended lectures by members of different research groups at Nevis Laboratories, worked on research projects, and presented oral reports on their progress at the end of the 10-week program. Among other activities, the students received a seminar about RARAF and took a tour.

This year Margo Kinneberg of Vassar College, Poughkeepsie, NY participated in the program and worked with Sasha Lyulko on imaging and analyzing micronuclei in irradiated lymphocytes.

We are initiating our first RARAF Microbeam Training Course, to be held in the Spring of 2011. The training course will be designed to give interested physicists and biologists a thorough and hands-on introduction to microbeam technology. Potential

participants were notified by fliers as well as posted and verbal announcements at the Radiation Research Society meeting held in September and by e-mail, using an address list from the most recent Microbeam Workshop, held in 2009. Seventeen applications with CVs were received. The applicants were from the U.S., Europe, South America and the mid-East and had a wide range of education levels and experience, from undergraduate degree to post-doc to researcher. The applicants were about evenly split on gender and background: radiobiology or physics. Of these applicants, a class of 6 was selected. The students will receive lectures on microbeam physics and biology, view demonstrations of the procedures used to validate the microbeam size and position and the biological procedures used to prepare cells for irradiation, and will plate and irradiate cells with the microbeam themselves.

**Dissemination**

The content of our website is continually updated to reflect the current state of the research at RARAF. For regular users we offer useful information such as the current month’s accelerator schedule, information on experiment scheduling, and our experiment scheduling form. For prospective new users there is a significant amount of information about the work done at RARAF and the capabilities of the facility, as well as forms and instructions for proposing new experiments. In the Dissemination section, we offer a list of papers detailing research performed at RARAF and published in peer-reviewed journals. Many of these papers and almost all recent papers are available in PDF format free from our web site. The web site also has information on the Slow and Fast Neutron and Charged Particle beams that are available for those interested. To further disseminate general information about microbeam technology, we are active participants in Wikipedia. We have created or significantly expanded encyclopedic entries for a number of topics such as microbeam, RARAF, and Mirau interferometry and have encouraged others in the microbeam community to participate in these efforts as well.

The 10th International Workshop: Microbeam Probes of Cellular Radiation Response will be hosted at Columbia University in March 2012 by RARAF personnel. This workshop provides a forum for the microbeam community to come together and discuss the present and future of microbeam research. The RARAF web site will be the central repository for information on this meeting.

**Personnel**

The Director of RARAF is Dr. David Brenner, the Director of the Center for Radiological Research (CRR). The accelerator facility is operated by Mr. Stephen Marino, the manager, and Dr. Gerhard Randers-Pehrson, the Associate Director of RARAF.

Dr. Charles Geard, the former Associate Director of the CRR, now spends most of his time at RARAF.

Dr. Brian Ponnaiya, an Associate Research Scientist, is the biology advisor for RARAF. He presently spends about half his time at the CRR

Dr. Alan Bigelow, an Associate Research Scientist, is continuing the development of the multiphoton microscopy system and the “microspot” irradiation facility as well as Optical Electronic Tweezers for manipulating cells.

Dr. Guy Garty, a Research Scientist, finished developing the permanent magnet microbeam (PMM) and is now developing the Flow and Shoot (FAST) system. He spends about half his time working on the National Institute of Allergy and Infectious Diseases (NIAID) project, for which he is the project manager.

Dr. Antonella Bertucci, a Postdoctoral Fellow, spends part of her time at RARAF working on small animal irradiation using the microbeam

Dr. Andrew Harken, a Postdoctoral Fellow, is responsible for the x-ray microbeam and the Point and Shoot targeting system. He is also working on the imaging of cells without stain using a highly sensitive EMCCD camera.

Dr. Yanping Xu, a Postdoctoral Fellow, has been working on the development of a neutron microbeam. He is also working on the NIAID project, developing an accelerator-generated neutron source with a spectrum similar to that at Hiroshima.

Sasha Lyulko, a graduate student in the Physics Department at Columbia University, is involved in developing the Simultaneous Immersion Mirau Interferometry (SIMI) system and also spent about half her time working on imaging on the NIAID project.

Dr. Stephane Lucas, a visiting professor, who arrived in September, 2009 on a sabbatical leave from the University of Namur, Belgium, stayed until May. Three students from the University of Namur visited RARAF and performed cell irradiations using the Track Segment Facility while he was here.

Dr. Alexandre Mezentsev, an Associate Research Scientist, irradiated cultured tissue systems using the Track Segment Facility and spent a portion of his time at RARAF. He left the CRR in August.

3. Hei, T.K., Zhou, H., Chai, Y., Ponnaiya, B., and Ivanov, V.N. Radiation Induced Non-targeted Response: Mechanism and Potential Clinical Implications. *Curr. Mol. Pharmacol.* 2010 Dec 14. [Epub ahead of print].
4. Hong, M., Xu, A., Zhou, H., Wu, L., Randers-Pehrson, G., Santella, R.M., Yu, Z. and Hei, T.K. Mechanism of genotoxicity induced by targeted cytoplasmic irradiation. *Br J Cancer.* **103**: 1263-1268 (2010) PMID: PMC2967061.
5. Ivanov, V.N., Zhou, H., Ghandhi, S.A., Karasic, T.B., Yaghoubian, B., Amundson, S.A. and Hei, T.K. Radiation-induced bystander signaling pathways in human fibroblasts: a role for interleukin-33 in the signal transmission. *Cell. Signal.* **22**: 1076-87 (2010) PMID: PMC2860693.
6. Kovalchuk, O., Zemp, F., Filkowski, J., Altamirano, A., Dickey, J.S., Jenkins-Baker, G., Marino, S.A., Brenner, D.J., Bonner, W.M. and Sedelnikova, O.A. MicroRNAome changes in bystander three-dimensional human tissue models suggest priming of apoptotic pathways. *Carcinogenesis* 31: 1882-1888 (2010) PMID: PMC2950932.
7. Lyulko, O.V., Randers-Pehrson, G. and Brenner, D.J. Immersion Mirau interferometry for label-free live cell imaging in an epi-illumination geometry. In: *Imaging, Manipulation, and Analysis of Biomolecules, Cells, and Tissues VIII*, Daniel L. Farkas, Dan V. Nicolau and Robert C. Leif, eds. *Proceedings of SPIE Vol. 7568*, SPIE, Bellingham, WA, 2010.
8. Schettino, G., Johnson, G.W., Marino, S.A. and Brenner, D.J. Development of a method for assessing non-targeted radiation damage in an artificial 3D human skin model. *Int. J. Radiat. Bio.* **86**: 593-601 (2010).
9. Xu, Y., Randers-Pehrson, G., Marino, S.A., Bigelow, A.W., Akselrod, M.S., Sykora, J.G. and Brenner, D.J. An accelerator-based neutron microbeam system for studies of radiation effects. *Radiat. Prot. Dosimetry.* 2010 Dec 3. [PubMed in process]. ■

#### RECENT PUBLICATIONS OF WORK PERFORMED AT RARAF

1. Ghandhi, S.A., Ming, L., Ivanov, V.N., Hei, T.K. and Amundson, S.A. Regulation of early signaling and gene expression in the alpha-particle and bystander response of IMR-90 human fibroblasts. *BMC Med. Genomics* **3**: 31 (2010) PMID: PMC2919438.
2. Ghandhi, S.A., Sinha, A., Markatou, M., and Amundson, S.A. Time-series clustering of gene expression in irradiated and bystander fibroblasts: an application of FBPA clustering *BMC Genomics* **12**: 2 (2011) PMID: PMC3022823.



Dr. Yanping Xu, Postdoctoral Research Scientist at RARAF.